water

MDPI

Article

Valorization of Invasive *Faxonius limosus* Shell Waste as a Biosorbent for Zn(II) and Cd(II) Removal from Aqueous Solutions

Vesna Vasić [1,*], Dragana Lukić [1,*], Teodora Subić [1], Nenad Popov [2], Jelena Lubura Stošić [1], Oskar Bera [1] and Ivana Čabarkapa [3]

[1] Faculty of Technology Novi Sad, University of Novi Sad, Bulevar cara Lazara 1, 21000 Novi Sad, Serbia; subic.99.19.b@uns.ac.rs (T.S.); jelenalubura@uns.ac.rs (J.L.S.); obera@uns.ac.rs (O.B.)
[2] Scientific Veterinary Institute "Novi Sad", 21000 Novi Sad, Serbia; nenad.p@niv.ns.ac.rs
[3] Institute of Food Technology in Novi Sad, University of Novi Sad, 21000 Novi Sad, Serbia; ivana.cabarkapa@fins.uns.ac.rs
* Correspondence: vesna.vasic@uns.ac.rs (V.V.); dkukic@uns.ac.rs (D.L.)

Abstract

The increasing contamination of aquatic environments by heavy metals and the need for sustainable management of invasive aquatic species have stimulated interest in low-cost biosorbents derived from biological waste. In this study, minimally processed shells of the invasive crayfish *Faxonius limosus* were evaluated for Zn(II) and Cd(II) removal from aqueous solutions. FTIR, SEM, and BET/BJH analyses revealed an organic-mineral material containing amino, hydroxyl, amide, and carbonate functional groups with a predominantly mesoporous structure. Batch experiments showed rapid metal uptake, with equilibrium reached within approximately 60 min. The pseudo-second-order model provided the best fit to the kinetic data, while equilibrium behavior was best described by the Temkin model for Zn(II) and the Langmuir model for Cd(II). Langmuir maximum adsorption capacities were 70.69 mg/g for Zn(II) and 302.12 mg/g for Cd(II). Metal removal was influenced by both initial pH and biosorbent dose, with 2.5 g/L providing high removal efficiencies for both metals. Calcium-release experiments showed increased Ca concentrations in the presence of Zn(II) and Cd(II), supporting the involvement of the Ca-rich mineral fraction in metal removal. Overall, *F. limosus* shell waste represents a promising low-cost biosorbent and a sustainable valorization route for invasive biomass.

Keywords: biosorbents; invasive species; *F. limosus*; heavy metals; crayfish shells

Check for updates

Academic Editors: Xiaochun Yin and Yongfeng Zhu

Received: 5 June 2026
Revised: 12 October 2026
Accepted: 14 October 2026
Published: 15 October 2026

Copyright: © 2026 by the authors. Licensee MDPI, Basel, Switzerland. This article is an open access article distributed under the terms and conditions of the Creative Commons Attribution (CC BY) license.

1. Introduction

Heavy metal contamination of aquatic environments has become a major environmental concern as a consequence of intensified industrialization and the continuous discharge of effluents containing heavy metals from sectors such as mining, metallurgy, electroplating, fertilizer and pesticide production, food processing, and pharmaceutical manufacturing. Unlike many organic pollutants, heavy metals are not biodegradable and can persist in aquatic systems, accumulate in sediments and biota, and subsequently enter the food chain, posing long-term ecological and human health risks [1]. Because of their persistence, toxicity, and ecological impacts, these metals are considered major contributors to ecosystem degradation and are routinely monitored as priority pollutants worldwide [2]. Particular attention has been given to Zn(II) and Cd(II), which are frequently detected in contaminated

waters. Although zinc is recognized as an essential micronutrient involved in numerous biological processes, its presence at elevated concentrations may cause harmful effects, including gastrointestinal disorders, skin irritation, fever, and hematological disturbances. Cadmium is of particular concern because of its high toxicity and bioaccumulation potential, making its occurrence in aquatic systems problematic even at low concentrations [3]. Cadmium is introduced into surface waters through mining and metallurgical activities, battery manufacturing, electroplating, pigment production, phosphate fertilizers, and industrial wastewater discharges. Zinc, although less toxic than cadmium, may also exert harmful effects at elevated concentrations, causing toxicity to aquatic biota and disrupting ecological balance. Furthermore, the simultaneous presence of these metals in contaminated waters represents a challenge for water treatment and environmental protection. For these reasons, the development of efficient, low-cost, and sustainable materials for their removal from water remains of significant scientific and practical interest.

Conventional treatment methods for heavy metal-contaminated water can be effective, but they are often associated with high operational costs, sludge generation, and reduced efficiency at low pollutant concentrations. For this reason, biosorption has attracted increasing attention as a low-cost and environmentally friendly alternative. Biosorption can remove metal ions through a combination of ion exchange, surface complexation, electrostatic attraction, and precipitation, while using abundant biological materials or waste-derived sorbents [1,4]. Crustacean shell waste is particularly promising in this context because it contains chitin, proteins, and calcium carbonate, all of which provide functional groups and mineral phases favorable for metal binding.

At the same time, the management of invasive aquatic species represents another important environmental challenge. The Intergovernmental Science Policy Platform on Biodiversity and Ecosystem Services (IPBES) [5] has identified Invasive Alien Species (IAS), organisms introduced by humans into regions beyond their natural range, as one of the five primary direct drivers of global biodiversity loss. IPBES emphasizes that invasive species represent one of the most serious threats to biodiversity and human well-being in the coming decade. As stated in the EU Biodiversity Strategy for 2030 [6], invasive alien species can severely compromise efforts to protect and restore natural ecosystems. In addition to causing extensive harm to biodiversity and the economy, many of these species also contribute to the emergence and spread of infectious diseases, endangering both humans and wildlife. Their introduction rate has risen markedly in recent years. In Europe alone, 354 of the 1872 species currently classified as threatened are impacted by invasive alien species. Without effective prevention and control measures, the pace of invasion and the associated risks to nature and human health will continue to escalate. The implementation of the EU Invasive Alien Species Regulation [7], along with other relevant legislation and international agreements, must be further strengthened. These efforts should focus on minimizing, and where possible, preventing the introduction and establishment of alien species within the EU environment. The overarching goal is to effectively manage established invasive alien species and reduce the number of Red List species currently threatened by them by 50%.

The spiny-cheek crayfish *Faxonius limosus* (Rafinesque, 1817), also known as *Orconectes limosus*, belongs to the largest crayfish family, *Cambaridae*, which includes 14 genera and 441 species. Native to North and Central America, it was the first non-native crayfish species introduced into Europe. The only recorded successful introduction occurred in 1890, when 90 individuals supplied by the US Commission of Fish and Fisheries were released into a fishpond in western Poland. Since then, the species has spread widely and is now present in rivers, canals, and lakes across 23 European countries [8]. It is an omnivorous species that feeds on aquatic plants, fish eggs, and various invertebrates, thereby negatively

impacting biodiversity. Moreover, it serves as a carrier of the crayfish plague, a disease fatal to native European crayfish. Through its extensive burrowing activity, it can also destabilize riverbanks and alter aquatic habitats. Since its introduction, *F. limosus* has become the most widespread non-indigenous crayfish species in Europe and is now listed among the invasive alien species (IAS) of Union concern under EU Regulation 2016/1141 [9]. *Faxonius limosus* is adaptable to a wide variety of environmental conditions and is an active migrator that can live and reproduce in brackish waters with salinity up to 10% [10]. Taking into account the above, there is an urgent need to monitor and prevent its further spread in the inland waters of Serbia and the Danube River Basin, in order to address the problem of its impact on biodiversity. The first record of *F. limosus* in Serbia dates back to 2002, when it was observed in the Danube River near Apatin. Since then, the species has expanded its distribution throughout the entire section of the Danube, the Sava, Tisa, Velika Morava, and Tamiš rivers [11].

The aim of this study was to investigate the potential use of *Faxonius limosus* crayfish shells as a biosorbent for the removal of zinc and cadmium ions from water. After crayfish were collected from various locations along the course of the Danube River in Serbia and the meat was separated, a large amount of shell waste remained and was utilized in this research. Batch adsorption experiments were conducted to investigate the removal efficiency of Zn(II) and Cd(II) from model aqueous solutions using the prepared material, whereas the adsorption behavior was further interpreted through kinetic and isotherm modeling. Given the substantial quantities of this type of waste generated worldwide, its application as a biosorbent has been the subject of increasing research interest in previous years. Several studies have demonstrated the potential of crayfish shells and crayfish-shell-derived materials for the removal of heavy metals from aqueous solutions [12,13]. More recent studies have predominantly focused on thermally or chemically modified crayfish-shell-derived materials, particularly biochars, to enhance their sorption properties [14,15]. In contrast, considerably less attention has been given to the direct use of minimally processed crayfish shell biomass as a biosorbent.

This study contributes to the growing field of waste-derived biosorbents by evaluating minimally processed shell waste as a low-cost material for Zn(II) and Cd(II) removal. Unlike many recently investigated crayfish-shell-derived adsorbents, the material was used without chemical modification, activation, or conversion into biochar. In addition, while the adsorption potential of shells from several crayfish species has previously been investigated, to the best of our knowledge, the adsorption properties of *Faxonius limosus* shells have not yet been specifically evaluated. This provides an additional rationale for investigating the potential valorization of shell biomass generated during the management of this invasive species.

2. Materials and Methods

2.1. Preparation of the Adsorbents

Crayfish shells obtained after meat separation were washed several times with pure water to remove remaining dirt, flesh, and other impurities that may have remained on the surfaces of the shells. The shells were dried in a laboratory oven ((Memmert GmbH + Co. KG, Schwabach, Germany)) at 105 °C for 24 h, after which they were sun-dried for an additional 48–72 h. The dried crayfish shells were ground using an electric coffee grinder and subsequently sieved through a mesh with an aperture size of 0.4 mm, and the fraction with particle sizes smaller than 0.4 mm was subsequently used in all further experiments.

2.2. Characterization of the Adsorbents

Comprehensive characterization of the adsorbent is essential to assess its physicochemical properties that may influence the adsorption process. In particular, the potential release of pollutants from the adsorbent into the aqueous phase may pose environmental risks, especially when organic matter is present. For this reason, the chemical oxygen demand (COD) was determined in water after 24 h of contact with the adsorbent to assess the possible release of organic compounds from the crayfish shell material into the aqueous phase during its application as a biosorbent. The analysis was performed using potassium dichromate as the oxidizing agent, following the standard dichromate reflux method [16]. Surface functional groups of the investigated crayfish shell particles were identified by Fourier Transform Infrared (FTIR) spectroscopy operated in non-contact external reflection mode. Spectra were recorded over the wavenumber range of 400–4000 cm^{-1} at a resolution of 4 cm^{-1} using an Alpha FTIR spectrometer (Bruker Optics GmbH & Co. KG, Ettlingen, Germany). The surface morphology of the crayfish shells was examined by scanning electron microscopy (SEM) using a JEOL JSM-6460LV (JEOL Ltd., Akishima, Tokyo, Japan) scanning electron microscope and INCA X-sight software (Oxford Instruments, Abingdon, UK). The point of zero charge (pH_{PZC}) of the crayfish shell biosorbent was determined using the pH drift method according to Smičiklas et al. [17]. Briefly, 0.25 g of the adsorbent was added to 50 mL of 0.1 M KNO_3 solution with initial pH values adjusted between 1 and 12 using 0.1 M HNO_3 or 0.1 M KOH. The suspensions were shaken for 24 h at room temperature to allow equilibration between the solid and liquid phases. Subsequently, the adsorbent was separated by filtration, and the final pH of each solution was measured. The pH_{PZC} value was determined from the plateau region of the plot relating the initial and final pH values. The specific surface area and pore-size distribution of crayfish shells were determined using a gas sorption analyzer (Anton Paar QuantaTec Inc., Boynton Beach, FL, USA)). The specific surface area was calculated using the Brunauer–Emmett–Teller (BET) method, while the pore-size distribution was derived from the desorption branch of the nitrogen adsorption–desorption isotherm applying the Barrett–Joyner–Halenda (BJH) model.

2.3. Batch Adsorption

Aqueous solutions of Cd(II) and Zn(II) were prepared by dissolving cadmium nitrate tetrahydrate ($Cd(NO_3)_2 \cdot 4H_2O$) and zinc sulfate heptahydrate ($ZnSO_4 \cdot 7H_2O$) in deionized water. Batch adsorption experiments were performed at room temperature using a laboratory orbital shaker (KS 260, IKA-Werke GmbH & Co. KG, Staufen, Germany). For the adsorption experiments, 0.25 g of adsorbent was mixed with 100 mL of metal ion solution at an initial pH of 5. For kinetic studies, the contact time ranged from 5 min to 24 h at a fixed initial metal ion concentration of 50 mg/L.

The effects of adsorbent dose and initial solution pH on Zn(II) and Cd(II) removal were investigated in separate batch experiments. The effect of adsorbent dose was evaluated at biosorbent concentrations of 1.0, 2.5, and 5.0 g/L, using an initial metal concentration of 50 mg/L and an initial pH of 5 and a contact time of 6 h. The influence of initial solution pH was investigated by adjusting the metal solutions to pH 3, 4, 5, 6, and 7 prior to the addition of the biosorbent, while the adsorbent dose, initial metal concentration (50 mg/L), contact time (6 h), and temperature were kept constant. Isotherm experiments were carried out by varying the initial metal ion concentration from 10 to 500 mg/L for Zn ions and 700 mg/L for Cd ions, while maintaining a constant contact time of 6 h. Upon completion of the adsorption period, the solid phase was separated by filtration through MN 85/70 BF membrane filters (MACHEREY-NAGEL GmbH & Co. KG, Düren, Germany) with a pore size of 0.45 μm. The concentrations of metal ions in the aqueous phase before (C_0) and

after adsorption (C) were quantified in the filtrate using inductively coupled plasma mass spectrometry (ICP-MS; Agilent 7700x, Agilent Technologies, Santa Clara, CA, USA) [18]. The adsorption capacity (q) and adsorption efficiency (E) of metal ions were calculated based on the following equations:

$$q = (C_0 - C)/m \quad (1)$$

$$E = (C_0 - C)/C_0 \cdot 100 \quad (2)$$

Here, m is the mass of added adsorbent per liter of solution.

2.4. Adsorption Kinetic Models

Adsorption kinetics provides insight into the rate- and time-dependent behavior of the adsorption process, including changes in solute uptake over time, the effect of mass transfer on the adsorption process, and the overall efficiency of the investigated adsorbent. Kinetic analysis describes this change in uptake over time and contributes to a better understanding of adsorption behavior by allowing comparison of apparent uptake rates and the time required to approach a stable adsorption capacity. However, commonly used kinetic models should not be used as direct evidence of a specific mechanism or rate-controlling step [19–21]. In this study, the experimental kinetic data were fitted using commonly applied batch kinetic models, including the pseudo-first-order (PFO), pseudo-second-order (PSO), and Elovich models to characterize the temporal uptake behavior and assess the possible contribution of surface uptake. The resulting parameters were interpreted together with equilibrium data, material characterization, and other experimental evidence to develop a more comprehensive interpretation of the adsorption mechanism.

The pseudo-first-order (PFO) kinetic model describes adsorption as a reversible process and assumes that the rate of occupation of adsorption sites is proportional to the number of unoccupied sites. The differential form of the model is expressed as follows [22]:

$$\frac{dq_t}{dt} = k_1(q_e - q_t) \quad (3)$$

Here, q_e (mg/g) and q_t (mg/g) represent the adsorption capacities at equilibrium and at time t, respectively, and k_1 (min^{-1}) is the pseudo-first-order rate constant.

The pseudo-second-order (PSO) kinetic model assumes that adsorption proceeds via chemisorption involving both adsorption and ion-exchange mechanisms on the adsorbent surface, with chemical interaction at the active sites being the rate-limiting step [22]. The differential form of the PSO model is expressed as follows:

$$\frac{dq_t}{dt} = k_2(q_e - q_t)^2 \quad (4)$$

Here, k_2 (g/mg min) is the pseudo-second-order rate constant. Integration of the above equation under the initial condition $q_t = 0$ at $t = 0$ yields the following expression:

$$q_t = \frac{q_e^2 k_2 t}{1 + q_e k_2 t} \quad (5)$$

The Elovich kinetic model is widely applied to describe chemisorption processes on solid surfaces, particularly for systems characterized by heterogeneous adsorption sites. This empirical model assumes that the adsorption rate decreases exponentially with

increasing surface coverage as a consequence of progressive occupation of energetically less favorable sites [22,23]. The Elovich equation is expressed as follows:

$$\frac{dq_t}{dt} = \alpha \exp(-\beta q_t) \quad (6)$$

Here, α (mg/g min) represents the initial adsorption rate, and β (g/mg) is a constant related to surface coverage and the activation energy of chemisorption.

2.5. Adsorption isotherm Models

To elucidate the adsorption mechanism of Zn(II) and Cd(II) ions onto the surface of crayfish shells, the experimental equilibrium data were interpreted using widely applied adsorption isotherm models, Langmuir, Freundlich, and Temkin. These models provide insight into the adsorption behavior and surface characteristics of the adsorbent. The corresponding isotherm equations were applied in their original nonlinear form to facilitate parameter estimation and enable straightforward comparison of model performance.

The Langmuir isotherm model assumes monolayer adsorption on a homogeneous surface with a finite number of identical and energetically equivalent adsorption sites, and no interaction between adsorbed species. Once an adsorption site is occupied, no further adsorption can occur at that site [24]. The nonlinear form of the Langmuir equation is expressed as follows [25]:

$$q = \frac{q_L K_L C}{1 + K_L C} \quad (7)$$

Here, q_l (mg/g) is the maximum monolayer adsorption capacity, and K_L (l/g) is the Langmuir constant.

The Freundlich isotherm is an empirical model that does not rely on a specific theoretical assumption of adsorption and is commonly used to describe adsorption on heterogeneous surfaces [26]. The model incorporates two fitting parameters, K_F and n, which are related to the adsorption capacity and adsorption intensity, respectively, and are expressed as follows:

$$q = K_F C^{1/n} \quad (8)$$

Here, K_F is the Freundlich constant ((mg/g)/(l/mg)$^{1/n}$), and $1/n$ is a constant related to the RC surface heterogeneity.

The Temkin isotherm model is a two-parameter model derived from theoretical considerations of adsorption. It describes adsorption on heterogeneous surfaces while accounting for the effects of indirect adsorbate-adsorbent interactions on the adsorption process. In this model, the heat of adsorption is assumed to decrease linearly with increasing surface coverage due to these interactions [24,27]. The Temkin isotherm equation is expressed as follows [23]:

$$q = \frac{RT}{b_T} \ln(A_T C) \quad (9)$$

Here, R is the ideal gas constant (8.314 J/mol K), T is the temperature (K), A_T (l/mg) is the Temkin isotherm constant, and b_T (J/mol) is a constant related to the heat of adsorption.

3. Results

3.1. Characterization of the Adsorbent

To assess the potential release of organic matter from the crayfish shell biosorbent during its application, the chemical oxygen demand (COD) of water after 24 h of contact with the adsorbent was determined. The obtained value of 60.14 mg O_2/L indicates a certain release of organic compounds into the aqueous phase, which can be attributed to the presence of residual proteins, chitin-derived components, and other nat-

urally occurring organic constituents of the shell matrix. The measured COD value remained below the limit value of 125 mg O_2/L commonly prescribed for treated municipal wastewater discharges [28]. This indicates that the release of organic matter from the crayfish shell biosorbent was relatively moderate and is unlikely to represent a major environmental concern.

Due to their chemical composition, characterized by a high content of calcium carbonate, chitin, proteins, and pigments, as well as a nanoporous structure, crustacean shell waste exhibits considerable potential as an adsorbent. This specific composition directly contributes to favorable adsorption performance, as the presence of various active sites and functional groups enhances interactions with target contaminants. FTIR spectroscopy was employed for the rapid identification of the chemical composition of the obtained shell powders. Scanning electron microscopy (SEM) was used to examine the surface morphology and microstructural features of the shell powder.

3.2. Functional Groups

The FTIR spectrum recorded for the crayfish shells is given in Supplementary Figure S1: FTIR spectra of *F. limosus* crayfish shells. Table 1 shows peaks obtained from the FTIR analysis.

Table 1. Peaks obtained from the FTIR analysis.

ν (cm^{-1})	Interpretation
3269.9	O-H/N-H stretching (H-bonded)
2920.35, 2851.08	C-H of CH_2/CH_3
1633.28	Amide I (C=O stretch)
1537.68, 1514.80, 1505.18	Amide II (N-H bend + C-N stretch)
1393.56	CH_3 symmetric deformation and/or CO_3^{2-}
1257.21	Amide III (C-N stretch + N-H bend)
1153.21	(C-O-C) glycosidic bridge
1065.41, 1027.41	C-O/C-N stretching, ring vibrations
860.51	CO_3^{2-}

The FTIR spectrum confirmed chitin (1153, 1065, 1027, 1257 cm^{-1}) [29–31] interlaced with proteins (amide I/II at ~1633 and 1540–1505 cm^{-1}) [30,32]. The carbonate band near 860 cm^{-1} confirms the presence of a mineral phase ($CaCO_3$) [31]; the position suggests a significant aragonite or amorphous $CaCO_3$ component, rather than purely calcite. The broad 3269 cm^{-1} band [29,31,33] and the 1633 cm^{-1} shoulder imply bound water and hydrogen bonding [30,32]. Similar spectral features have been reported for crustacean shell-derived biosorbents in previous studies [29,30,32,33], which have confirmed the presence of characteristic chitin and calcium carbonate ($CaCO_3$) components, along with their associated functional groups. The FTIR spectra typically reveal bands corresponding to amide I and amide II groups originating from the chitin structure, as well as carbonate-related vibrations associated with $CaCO_3$. These functional groups are considered potential adsorption sites and may contribute to metal binding through mechanisms such as ion exchange, surface complexation, and electrostatic interactions.

3.3. Morphological Characteristics

The morphological characteristics of crayfish shells, evaluated by SEM, are presented in Figure 1. The micrographs revealed a heterogeneous and irregular surface morphology characterized by a rough and porous structure. Numerous cavities, cracks, and uneven surface features can be observed, while no uniformly distributed or regularly shaped pores were detected. The rough and fragmented surface structure may be favorable for

adsorption processes, as it increases the probability of interaction between metal ions and available active sites on the biosorbent surface. In addition, the presence of cavities and irregular depressions suggests the existence of accessible mesoporous regions, which can facilitate diffusion and mass transfer of ions during adsorption.

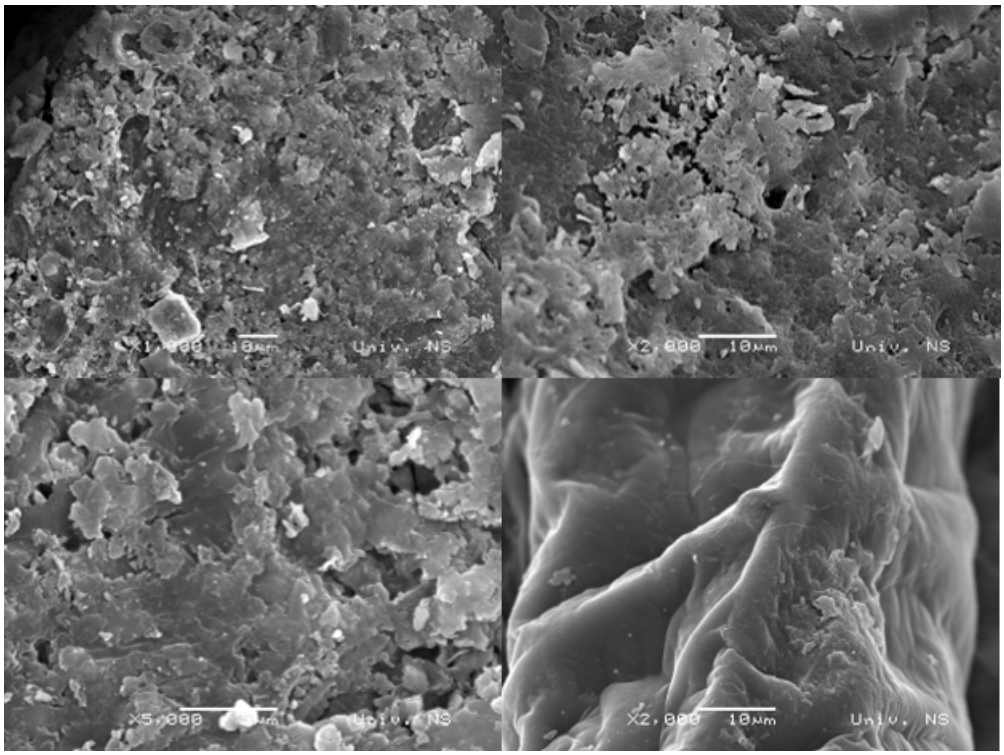

Figure 1. SEM image of *F. limosus* shells.

Figure 2 presents the nitrogen adsorption–desorption isotherm of the powdered river crayfish shell sample together with the pore-size distribution for pores below 100 nm, calculated from the desorption branch of the isotherm using the Barrett–Joyner–Halenda (BJH) method. The specific surface area of the material was determined based on the amount of nitrogen required for monolayer adsorption, while the main textural and porosity-related properties of the biosorbent are summarized in Table 2.

The relatively low BET specific surface area (2.094 m^2/g) suggests that adsorption is not governed primarily by extensive surface development but rather by the chemical composition of the shell material. The presence of calcium carbonate, which constitutes a major inorganic component of crustacean shells, may contribute to partial pore blockage and consequently limit the accessible surface area. Nevertheless, BJH analysis confirmed a mesoporous structure with a total pore volume of 3.327×10^{-3} cm^3/g for pores smaller than 30 nm and an average pore diameter of 3.18 nm. According to the IUPAC classification, these values indicate that the biosorbent belongs to the lower mesoporous range, which may facilitate the diffusion of metal ions toward the available adsorption sites.

Despite the relatively low specific surface area, the adsorption potential of crustacean shell-derived materials is often strongly influenced not only by textural properties, but also by the presence of functional groups such as amino, hydroxyl, and carbonate groups capable of interacting with metal ions through complexation, ion exchange, and electrostatic interactions. Therefore, the observed adsorption performance may be attributed to the combined effect of surface chemistry and mesoporous structure, which facilitates diffusion of metal ions toward the available active sites.

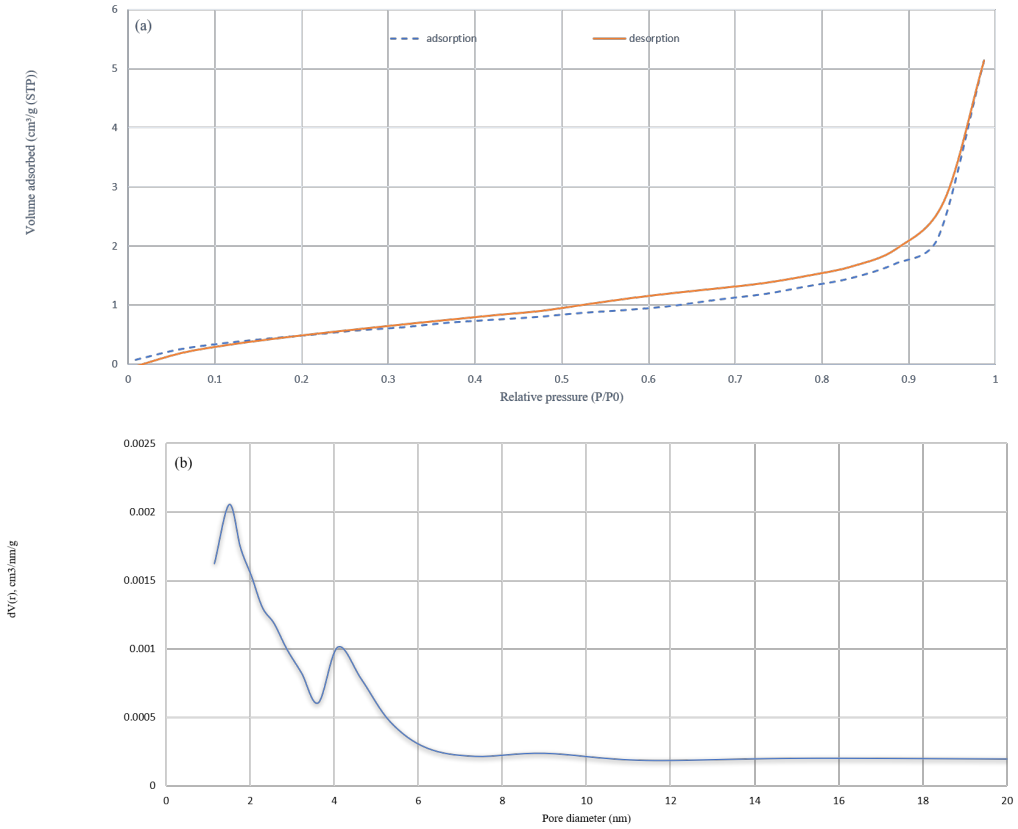

Figure 2. (**a**) Adsorption–desorption isotherms of crayfish shells and (**b**) pore-size distribution.

Table 2. Specific surface area of crayfish shells.

Material	Specific Surface Area S_{BET} (m^2/g)	Total Pore Volume for Pores Smaller Than 30 nm (cm^3/g)	Average Pore Diameter (nm)
Crayfish shell	2.094	3.3272×10^{-3}	3.1771

3.4. Adsorption Kinetics

Contact time is one of the most important operational variables affecting adsorption processes because it governs both the extent of pollutant removal and the overall treatment efficiency. For this reason, the adsorption of Zn(II) and Cd(II) ions onto the prepared crayfish shell biosorbent was monitored over time. As shown in Figure 3, both metal ions exhibited rapid adsorption during the initial stage of the process, with the highest uptake occurring within the first 30 min. This behavior is attributed to the abundance of readily accessible active sites on the biosorbent surface at the beginning of the adsorption. As these sites became progressively occupied, the adsorption rate decreased until equilibrium was established after approximately 60 min.

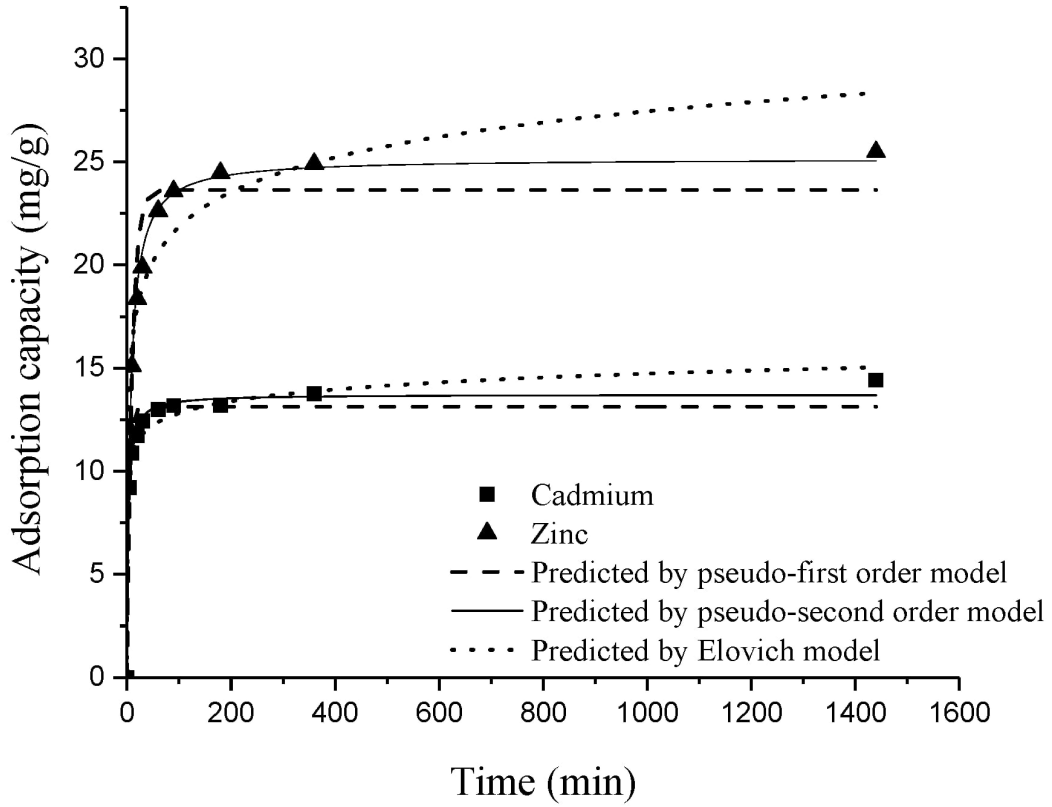

Figure 3. Effect of contact time on Cd(II) and Zn(II) biosorption by *F. limosus* shells under batch conditions (C_0 = 50 mg/L, t = 5 min–24 h, adsorbent dosage = 2.5 g/L, pH = 5.0, T = 25 ± 2 °C, agitation speed = 250 rpm).

The kinetic experimental data were fitted using the pseudo-first-order (PFO), pseudo-second-order (PSO), and Elovich kinetic models. The resulting kinetic parameters are presented in Table 3, while the corresponding model fits are shown in Figure 3.

Table 3. Kinetic parameters obtained by different kinetic models for Zn(II) and Cd(II) ions adsorption onto *F. limosus* shells.

Model	Parameter	Zn	Cd
Pseudo-first order	q_e (mg/g)	5.25	2.88
	k_1 (1/min)	0.0018	0.0012
	R^2	0.6015	0.699
Pseudo-second order	q_e (mg/g)	25.64	14.47
	k_2 (g/mg min)	0.0049	0.0088
	R^2	1	0.9998
Elovich	α (mg/(g min))	2.44	0.83
	β (g/mg)	4.45	5.74
	R^2	0.8533	0.8703

Although both Zn(II) and Cd(II) adsorption processes were best described by the pseudo-second-order kinetic model (Table 3), this result may be consistent with a mechanism that involves chemisorption. It should be noted that kinetic model fitting cannot definitively establish the adsorption mechanism. Differences in adsorption capacity and kinetic behavior were observed between the two metal ions, but they cannot be attributed solely to chemisorption based on model results.

According to the presented results (Figure 3), the higher adsorption capacity was obtained for Zn(II) (25.64 mg/g) compared to Cd(II) (14.47 mg/g). Similar trends have

been reported in the literature. Bahadir et al. [34] observed higher adsorption efficiencies for Zn(II) compared to Cd(II) on chitin-based shrimp shell waste, attributing this behavior to differences in metal-ligand interactions and hydration characteristics. Jaafarzadeh et al. [35] also reported superior kinetic fitting and high adsorption affinity for Zn(II) ions relative to other metal species when using chitin-derived biosorbents. Additionally, Vijayaraghavan et al. [36] demonstrated that Zn(II) adsorption onto crayfish shell particles proceeds more favorably than that of other divalent metal ions. Overall, the observed distinction between Zn(II) and Cd(II) adsorption behavior underscores the importance of metal-specific properties in governing adsorption performance and confirms that crustacean shell-derived biosorbents exhibit a higher selectivity toward Zn(II) ions under the investigated conditions.

3.5. Removal Efficiency

The removal efficiencies of Cd(II) and Zn(II) by the crayfish shell biosorbent showed distinct trends as a function of initial metal concentration. As shown in Figure 4, both metals exhibited high removal efficiencies at lower initial concentrations (10–50 mg/L), with Cd(II) removal ranging from 89.90% to 92.51% and Zn(II) removal from 83.71% to 92.00%. Within the investigated concentration range, the available adsorption sites were sufficient to accommodate most of the metal ions present, resulting in high removal efficiencies for both tested ions.

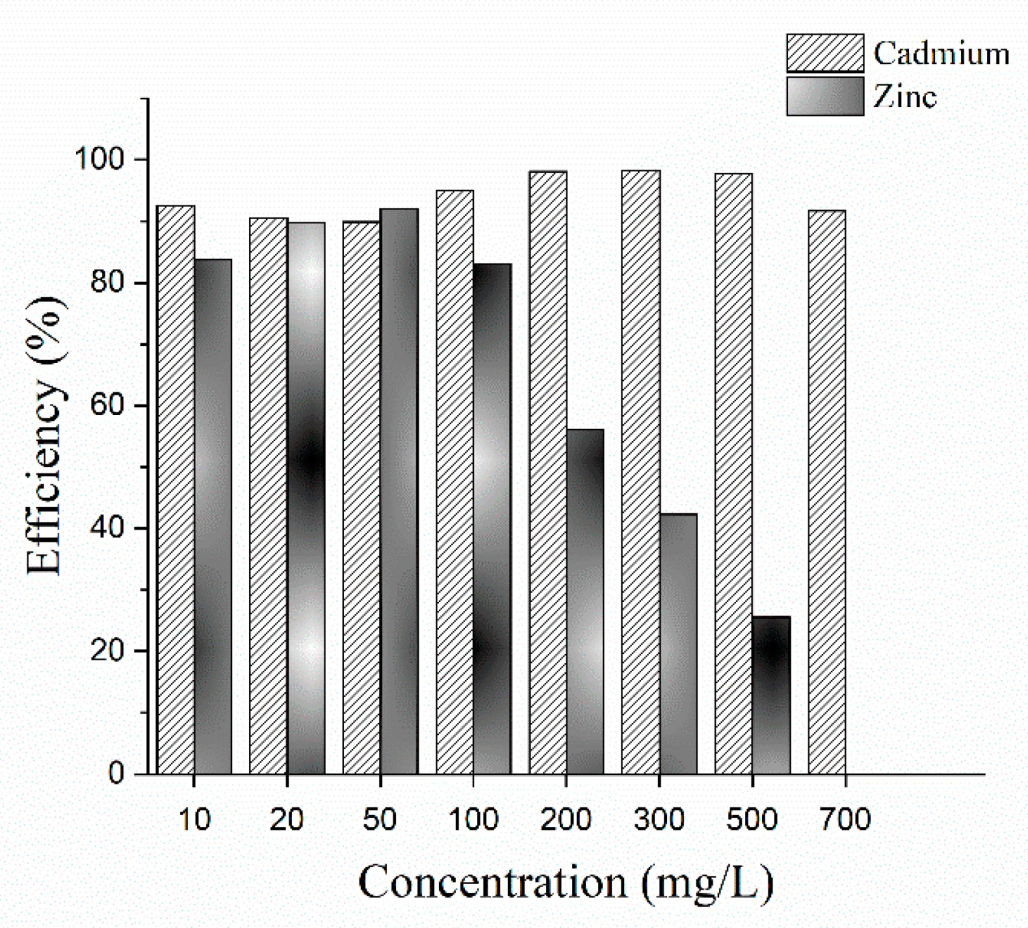

Figure 4. Removal efficiencies of Zn(II) and Cd(II) ions by *F. Limosus* shells under batch conditions (C_0 = 10–500 mg/L for Zn(II) and 700 mg/L for Cd(II), adsorbent dosage = 2.5 g/L, pH = 5.0, t = 6 h, T = 25 ± 2 °C, agitation speed = 250 rpm).

As the initial concentration increased, a clear divergence in behavior was observed. Cd(II) removal remained consistently high (90.55–98.31%), maintaining values above 97% even at 500 mg/L. This indicates a strong affinity of Cd(II) toward the functional groups present in the crayfish shell matrix (-N-H, -OH, and carbonate groups from $CaCO_3$). In contrast, Zn(II) removal efficiency declined significantly at concentrations >50 mg/L, despite the higher equilibrium capacity observed in kinetic experiments at C_0 = 50 mg/L.

These observations were further supported by changes detected in the FTIR spectra recorded before and after Zn(II) and Cd(II) adsorption. Noticeable variations in both band intensity and peak position suggested possible involvement of surface functional groups in the adsorption process (Figures S2 and S3 in the Supplementary). A broad absorption band observed in the region around 3200–3500 cm^{-1} was attributed to overlapping O-H and N-H stretching vibrations originating from hydroxyl and amino groups. Following Zn(II) and Cd(II) adsorption, a slight decrease in intensity accompanied by peak shifting was observed, indicating the participation of hydroxyl and amino functionalities in metal binding through complexation and electrostatic interactions. Furthermore, characteristic carbonate bands associated with calcium carbonate were detected in the region around 1400 cm^{-1} and below 900 cm^{-1}. Changes observed in these bands after adsorption suggest that carbonate groups may also contribute to Zn(II) and Cd(II) removal, likely through ion exchange mechanisms involving Ca^{2+} ions naturally present within the shell matrix. Overall, the observed FTIR spectral modifications suggest the possible involvement of amino, hydroxyl, and carbonate functional groups in the removal process. However, FTIR analysis cannot distinguish between direct surface complexation, ion exchange, or surface-induced precipitation. It also provides only qualitative evidence that these groups may play a role as binding sites, and should not be considered as definitive proof of the adsorption mechanism.

These findings are consistent with recent studies on chitosan- and crustacean-derived biosorbents, which confirm high efficiency and strong selectivity toward divalent heavy metals in single-component systems. For example, a recent study [37] reported removal efficiencies of up to ~92% for Zn(II) and ~86% for Cd(II) using functionalized chitosan nanocomposites, with adsorption following pseudo-second-order kinetics, indicating chemisorption as the dominant mechanism. Similarly, recent composite biosorbents based on chitosan derived from shrimp shells have demonstrated Cd(II) removal efficiencies around 80–85%, confirming the strong affinity of cadmium toward amino-functionalized surfaces and the spontaneous nature of the adsorption process [38]. These values are comparable to the lower concentration range observed in this study, while the significantly higher Cd(II) removal (>97% at high concentrations) suggests a particularly favorable interaction between Cd(II) and the crayfish shell matrix. It is acknowledged that the observed removal efficiencies may not be directly transferable to multi-metal or real wastewater matrices, where competing ions (e.g., Ca^{2+}, Mg^{2+}, Na^{+}) and natural organic matter could reduce available binding sites and adsorption capacity for Zn(II) and Cd(II) ions.

A recent study [39] further emphasizes that chitosan-based materials remain among the most effective low-cost biosorbents due to the abundance of -NH_2 and -OH functional groups, which enable strong coordination with metal ions. These functional groups facilitate inner-sphere complexation, which is typically more pronounced for Cd(II) than Zn(II), explaining the higher and more stable removal efficiencies observed for cadmium in the present study. In contrast, the decline in Zn(II) removal efficiency at higher concentrations aligns with recent findings showing that Zn adsorption is more sensitive to surface saturation and diffusion limitations. Studies on modified chitosan systems have shown that Zn(II) adsorption strongly depends on pH, surface functionalization, and available binding sites, and is often governed by weaker or more reversible interactions compared to Cd(II) [40].

3.6. Effect of Adsorbent Dose and Solution pH on Metal Uptake

In addition to contact time, additional experiments were performed to evaluate the influence of adsorbent dose and initial solution pH on the removal of Zn(II) and Cd(II). Increasing the amount of biosorbent resulted in a decrease in the adsorption capacity expressed per unit mass of material (Figure 5). The highest q_e values were obtained at the lowest tested dose (1 g/L), reaching approximately 63 mg/g for Zn(II) and 37 mg/g for Cd(II). At 2.5 g/L, these values decreased to approximately 30 and 15 mg/g, respectively, while a further increase in adsorbent dose to 5 g/L resulted in q_e values of approximately 15 mg/g for Zn(II) and 7 mg/g for Cd(II).

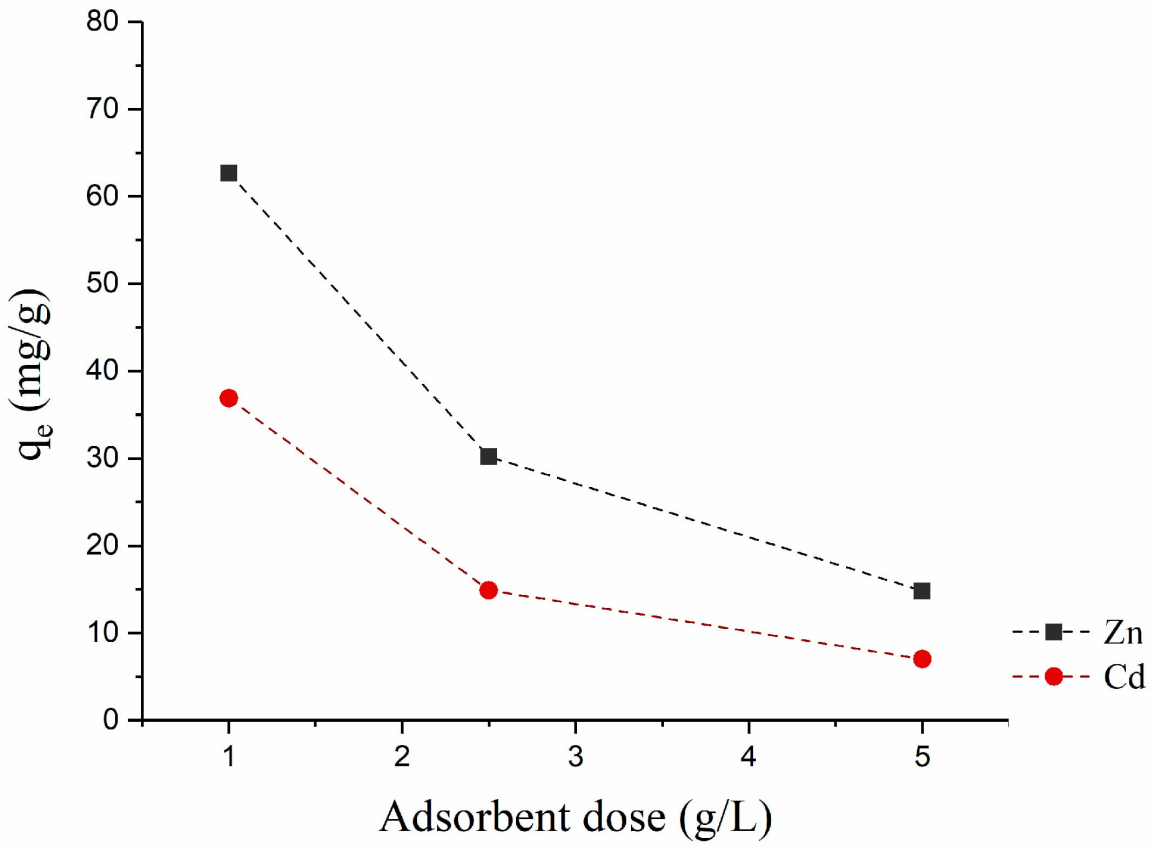

Figure 5. Effect of adsorbent dose on Cd(II) and Zn(II) removal from water.

However, the decrease in q_e with increasing adsorbent dose did not correspond to a proportional decrease in the overall metal removal efficiency. For Zn(II), removal efficiency increased from 76.97% at 1 g/L to 92.73% at 2.5 g/L and remained similarly high (91.09%) at 5 g/L. In contrast, Cd(II) removal was already very high at the lowest adsorbent dose, reaching 94.32% at 1 g/L, while efficiencies of 90.20% and 89.72% were obtained at 2.5 and 5 g/L, respectively. Thus, increasing the biosorbent dose improved Zn(II) removal up to 2.5 g/L, whereas no additional benefit was observed at 5 g/L. For Cd(II), the lowest investigated dose was already sufficient to achieve high removal efficiency. The decrease in adsorption capacity with increasing biosorbent dose can be attributed to the lower metal-to-adsorbent ratio. At lower doses, a greater amount of metal is available per unit mass of biosorbent, resulting in a higher proportion of occupied sorption sites and consequently higher adsorption capacity values. In contrast, as the biosorbent dose increases, the number of available binding sites becomes greater relative to the fixed amount of metal in solution. Similar dose-dependent behavior has been reported for other shell-based adsorbents. Fernández Pérez et al. [41] observed enhanced removal of Zn(II) and Cd(II) with increasing

dose of waste mollusk shells, demonstrating the influence of adsorbent dose on metal removal by $CaCO_3^-$ rich shell materials. Tizo et al. [42] similarly reported that increasing the amount of powdered eggshell enhanced Cd(II) removal efficiency, particularly at lower initial metal concentrations. Adeleke et al. [43] also identified adsorbent dose as one of the major process variables affecting Cd(II) uptake by an oyster shell-based biocomposite, with an optimized dose of approximately 2.53 g/L. These observations are consistent with the trends found in the present study, where increasing the amount of biosorbent favored overall metal removal but resulted in lower adsorption capacity per unit mass.

The initial pH of the solution is an important parameter controlling metal removal because it affects both the surface properties of the biosorbent and the chemical forms of metal ions present in solution. The effect of initial pH on Zn(II) and Cd(II) removal by *F. limosus* shell powder was therefore investigated over the selected pH range (Figure 6). The adsorption capacities remained relatively stable across the investigated conditions for both metals, although a moderate increase in Zn(II) removal was observed at the highest tested pH.

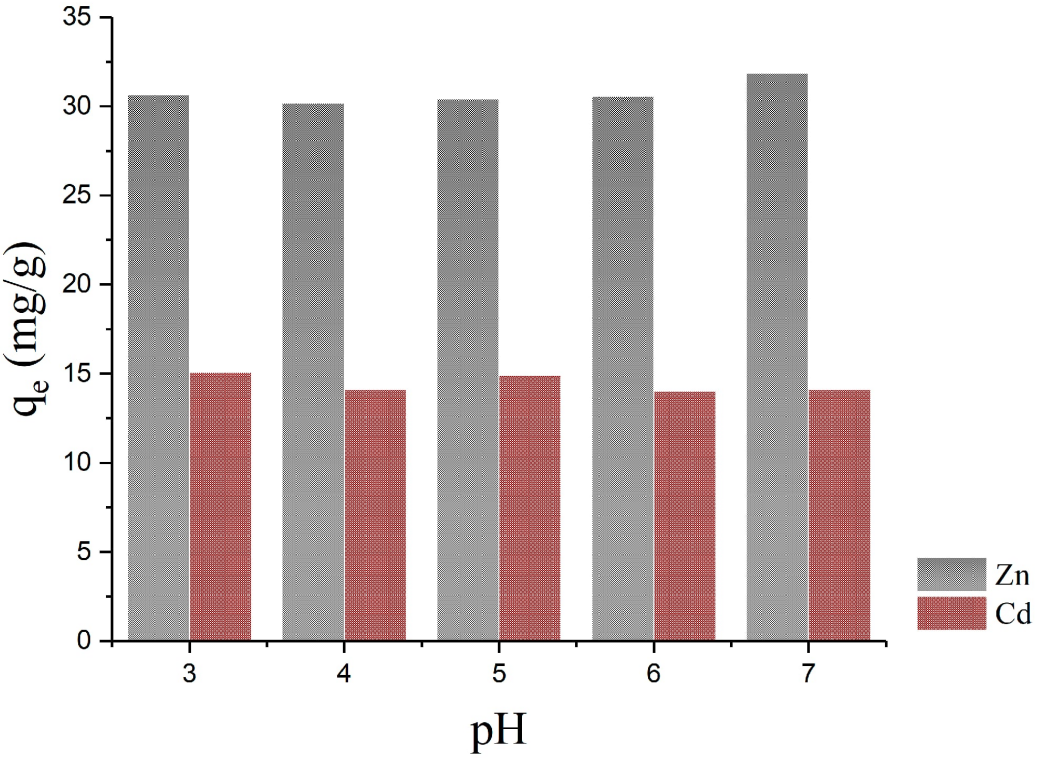

Figure 6. Effect of pH on Cd(II) and Zn(II) removal from water.

Similar pH-dependent behavior has been widely reported for Zn(II) and Cd(II) sorption, with favorable removal commonly observed around pH 5–6. For example, Lee et al. [44] reported maximum uptake of Zn(II) and Cd(II) at approximately pH 5 and selected this pH for subsequent adsorption experiments. Other studies have likewise reported pH 5 as a suitable operating condition for Cd(II) adsorption, primarily because competition with H^+ is reduced while precipitation-related interference can still be minimized [45]. However, the metal removal observed at elevated pH cannot be attributed exclusively to adsorption and should therefore be interpreted with caution, as precipitation may increasingly contribute to the overall removal process. With increasing pH, hydrolysis of Zn(II) and Cd(II) becomes increasingly important, which may result in the precipitation of their respective hydroxides. Consequently, the decrease in dissolved metal concentration measured after treatment may reflect a combination of adsorption and precipitation rather

than adsorption alone. Previous studies investigating Zn(II) and Cd(II) have specifically reported that precipitation at elevated pH can interfere with the interpretation of adsorption experiments. Lee et al. [44] observed that precipitation as insoluble $M(OH)_2$ became relevant at approximately pH 7 and emphasized that the resulting increase in apparent removal could no longer be attributed solely to sorption. Similarly, precipitation experiments have demonstrated that Zn(II) and Cd(II) removal by hydroxide formation increases markedly as pH approaches alkaline conditions, although the exact onset depends strongly on metal concentration and solution composition [46].

This consideration is particularly relevant for *F. limosus* shells because of their mineral fraction, including $CaCO_3$. Therefore, metal removal at higher pH cannot be attributed exclusively to adsorption on surface functional groups, and processes involving mineral dissolution, ion exchange, and precipitation may occur simultaneously. Accordingly, pH 5 was considered the most appropriate condition for the adsorption experiments in the present study. At this pH, Zn(II) and Cd(II) remain predominantly soluble under the investigated conditions, while competition from H^+ is lower than under more acidic conditions, allowing the adsorption performance of the shell material to be evaluated with a reduced risk of interpreting precipitation as adsorption.

The relatively limited variation in q_e observed within the investigated pH range further suggests that *F. limosus* shell powder can maintain substantial Zn(II) and Cd(II) removal under moderately acidic conditions. Based on these considerations, pH 5 was selected as an appropriate condition for evaluating the adsorption behavior of Zn(II) and Cd(II), as it provides favorable conditions for metal uptake while minimizing the potential contribution of hydroxide precipitation. The equilibrium behavior of both metals under the selected experimental conditions was further evaluated using adsorption isotherm models.

3.7. Adsorption Isotherm

The equilibrium adsorption behavior of Zn(II) and Cd(II) was evaluated using adsorption isotherm models, which provide insight into the interaction between the biosorbent and metal ions and enable estimation of the maximum adsorption capacity [47]. The effect of the initial metal concentration was investigated using Zn(II) solutions in the range of 10–500 mg/L and Cd(II) solutions in the range of 10–700 mg/L, whereas the contact time was maintained at 6 h throughout the experiments. As can be seen from Table 4 and Figure 7, the equilibrium adsorption behavior differed between the two metal ions. For Cd(II), the Langmuir isotherm exhibited the highest R^2 value (0.8889), indicating monolayer adsorption on a homogeneous adsorbent surface with finite, energetically equivalent binding sites [48]. For Zn(II), the Temkin model provided the best fit (R^2 = 0.9858), suggesting that adsorption occurs on a heterogeneous surface with significant adsorbate-adsorbent interactions and a linear decrease in the heat of adsorption with increasing surface coverage. The Langmuir model also showed a strong fit for Zn(II) (R^2 = 0.9766), indicating that monolayer coverage may coexist with heterogeneous energetic distributions. The superior fit of the Temkin model for Zn(II) implies that indirect interactions between adsorbed Zn(II) ions and the surface functional groups (-NH_2, -OH, C=O) contribute to the adsorption mechanism, whereas Cd(II) binding appears more consistent with ideal monolayer behavior. The dimensionless separation factor (R_l), derived from the Langmuir model, was used to assess whether adsorption was favorable under the investigated conditions. Values of R_L between 0 and 1 were obtained for all tested systems, confirming favorable adsorption of both metal ions under the studied conditions.

Table 4. Isotherm parameters for different models for Zn(II) and Cd(II) adsorption onto *F. limosus* shells.

Model	Parameter	Adsorbate	
		Zn	Cd
Langmuir	q_L (mg/g)	70.69	302.12
	K_L (L/mg)	0.066	0.083
	R_L	0.026–0.87	0.17–0.96
	R^2	0.9766	0.8889
Freundlich	K_F ((mg/g)(L/mg)$^{1/n}$)	13.37	49.65
	1/n	0.28	0.33
	R^2	0.9123	0.707
Temkin	b_T (J/mol)	201.985	45.139
	A_T (L/mg)	0.96	1.052
	R^2	0.9858	0.8264

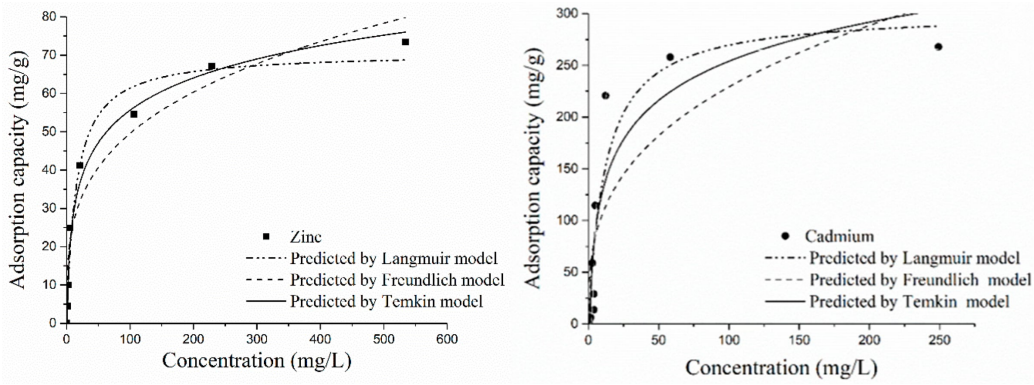

Figure 7. Experimental data and adsorption isotherms for Zn(II) and Cd(II) adsorption onto *F. limosus* shells under batch conditions (C_0 = 10–500 mg/L for Zn(II), C_0 = 10–700 mg/L for Cd(II), adsorbent dosage = 2.5 g/L, pH = 5.0, t = 6 h, T = 25 ± 2 °C, agitation speed = 250 rpm).

The maximum adsorption capacity for Zn(II) and Cd(II) predicted by the Langmuir model was 70.69 mg/g and 302.12 mg/g, respectively, which is in good agreement with the experimentally determined values of 73.4 mg/g for Zn(II) and 257.88 mg/g for Cd(II). These results are comparable to the literature data reported for crustacean-based biosorbents. For instance, Zhou et al. [13] reported adsorption capacities of 117 mg/g for zinc and 709 mg/g for lead ions using crayfish shell particles. In a related study [49], the same authors investigated Cd(II) adsorption onto raw crayfish shells, observing that the experimental data were best described by the Langmuir model, with the maximum adsorption capacity decreasing from 3.42 to 1.53 mmol/g as the biosorbent dosage increased from 0.4 to 3.2 g/L. Similarly, Jaafarzadeh et al. [50] examined Zn(II) removal using chitin derived from shrimp and crayfish shells, reporting maximum adsorption capacities of 270.27 mg/g and 181.18 mg/g, respectively, within the initial concentration range of 50–500 mg/L at pH 7. Rahman [51] investigated the adsorption of various heavy metals on modified shrimp-based chitosan and reported maximum adsorption capacities of 7.50 mg/g for zinc, 20.3 mg/g for copper, 15.0 mg/g for cadmium, and 76.34 mg/g for lead. In that study, high correlation coefficients (R^2 >0.98) for both Langmuir and Freundlich models indicated highly efficient adsorption behavior.

Overall, the obtained isotherm parameters indicate that *F. limosus* shells exhibit favorable adsorption characteristics for Zn(II) and Cd(II) ions, with adsorption behavior potentially governed by monolayer coverage on energetically equivalent binding sites,

consistent with findings reported for similar chitin- and calcium carbonate-based biosorbents. The isotherm models describe the equilibrium distribution but do not identify the mechanism. Thus, monolayer coverage should be interpreted as a mathematical construct rather than definitive evidence of a specific binding mode.

To evaluate the adsorption performance of *F. limosus* shells, the maximum adsorption capacities obtained in this study were compared with those reported for various crustacean shell-derived biosorbents, including raw shells, chitin, chitosan, and chemically modified materials, for the removal of Cd(II) and Zn(II) from single-metal solutions (Table 5), although direct comparison is not possible because of different experimental conditions that affect adsorption performance.

Table 5. Comparison of adsorption capacities for Cd(II) and Zn(II) removal using crustacean shell-derived biosorbents.

Biosorbent	Metal	q (mg/g)	C_0 (mg/L)	Dose (g/L)	pH	Reference
F. limosus shells	Cd(II)	302.12	10–700	2.5	5	This study
F. limosus shells	Zn(II)	70.69	10–500	2.5	5	This study
Chinese hairy shells	Zn(II)	117.0	40–140	1.6	5.5	Zhou et al. [13]
Clistocoeloma sinensis shells	Cd(II)	172	10–1100	1.6	5	Zhou et al. [49]
Chitin (shrimp shells)	Zn(II)	270.27	—	4	7	Jaafarzadeh et al. [50]
Chitin (crayfish shells)	Zn(II)	181.18	—	4	7	Jaafarzadeh et al. [50]
Modified shrimp chitosan	Zn(II)	7.50	—	—	—	Rahman [51]
Modified shrimp chitosan	Cd(II)	15.0	—	—	—	Rahman [51]
Callinectes sapidus shell	Zn(II)	185	10–2600	1	6	Morales-Barrera and Cristiani-Urbina [52]

F. limosus shells showed a much higher adsorption capacity than raw *Clistocoeloma sinensis* shells for Cd(II) at the same pH, despite a higher dose of biosorbent, indicating stronger Cd(II) binding by the *F. limosus* shell matrix. For Zn(II), the capacity of *F. limosus* shells (70.69 mg/g) was lower than values reported for *Chinese hairy* crab shells and *Callinectes sapidus* shells. However, these studies used lower adsorbent doses and different pH conditions, which can significantly affect the adsorption capacity. In addition, none of the studies reported removal efficiency percentages. In contrast, the present study provides complete efficiency data (Cd: 89.9–98.3%; Zn: 83.7–92.0% at $C_0 \leq 50$ mg/L), allowing a better assessment of the adsorption performance of *F. limosus* shells. Compared with chemically modified chitosan materials, *F. limosus* shells achieved much higher adsorption capacities while avoiding additional chemical processing steps.

The present study differs from previous work in several important aspects. *F. limosus* shells were used in a minimally processed form, without chemical modification or activation, providing a simple and low-cost approach to biosorbent preparation. Moreover, the use of shell waste generated from an invasive species offers an opportunity to combine invasive biomass management with the development of a value-added material for water treatment. The results demonstrate that effective removal of both metals can be achieved using minimally processed *F. limosus* shells, supporting their potential as a readily available biosorbent for metal-contaminated waters.

3.8. Calcium Release During Zn(II) and Cd(II) Removal

To further investigate the possible involvement of the Ca-rich mineral fraction of *F. limosus* shells in metal removal, Ca release into the solution was determined under the same experimental conditions used in the adsorption experiments (initial metal concentration of 50 mg/L, biosorbent dose of 2.5 g/L, and initial pH of 5). A control experiment containing the biosorbent and deionized water was performed under the same conditions. The mean

Ca concentration in the control was 50.85 mg/L, indicating that Ca-containing components of the shell are partially released into the aqueous phase even in the absence of Zn(II) and Cd(II). In the presence of metal ions, substantially higher Ca concentrations were measured, reaching 116.95 mg/L for Zn(II) and 92.90 mg/L for Cd(II). Thus, compared with the control, the presence of Zn(II) and Cd(II) resulted in an additional Ca release of approximately 66.1 and 42.1 mg/L, respectively.

The increased Ca release in the presence of both metal ions indicates that the Ca-rich mineral fraction of the shell participates in the metal-removal process. This observation is consistent with previous studies on $CaCO^{3-}$ rich shell materials. Fernández Pérez et al. reported the release of Ca^{2+} and other endogenous cations during the uptake of Zn(II), Cd(II), Cu(II), and Ni(II) by waste mollusk shells and related metal retention to interactions with the mineral fraction of the shell, including ion-exchange processes [41]. Similarly, $CaCO_3$ has been shown to contribute to metal removal through a combination of processes involving partial carbonate dissolution, ion exchange, and the formation of poorly soluble metal-containing phases. Wierzba et al. demonstrated that the role of $CaCO_3$ in metal removal cannot be described by a single mechanism, as its partial dissolution can influence ion-exchange equilibria while carbonate-related reactions may contribute to the precipitation of poorly soluble metal compounds [53].

The involvement of the carbonate fraction is particularly relevant for Cd(II). A recent study using scallop shells demonstrated that Cd uptake involved partial dissolution of shell $CaCO_3$, exchange between Ca and Cd, and subsequent nucleation of a $CdCO_3$ phase, illustrating the close relationship between Ca release and Cd removal in biogenic carbonate materials [54]. Therefore, the increased Ca concentrations observed during Zn(II) and Cd(II) removal provide additional experimental evidence for the involvement of the mineral component of *F. limosus* shells in the removal process. These findings also complement the adsorption results obtained in the present study. At a biosorbent dose of 2.5 g/L and an initial metal concentration of 50 mg/L, removal efficiencies of 92.73% for Zn(II) and 90.20% for Cd(II) were achieved. The simultaneous observation of high metal removal and enhanced Ca release supports the contribution of interactions between the dissolved metal ions and the Ca-containing shell matrix. However, since Ca release alone cannot distinguish between ion exchange, mineral dissolution, surface complexation, and subsequent precipitation processes, it should not be considered direct evidence of a single adsorption mechanism. Rather, together with the FTIR, pH-dependent adsorption, kinetic, and equilibrium results, the Ca-release experiments suggest that Zn(II) and Cd(II) removal by *F. limosus* shells results from the combined contribution of the organic and mineral components of the shell, with Ca-containing phases playing an important role in the overall uptake process.

3.9. Point of Zero Charge (pH_{PZC})

The point of zero charge (pH_{PZC}) of the *F. limosus* shell biosorbent is presented in Figure 8. The obtained value was 8.51, indicating that the adsorbent surface possesses a net positive charge at pH values below 8.51 and a net negative charge at pH values above this value. The relatively high pH_{PZC} can be attributed to the chemical composition of the crayfish shells, which are rich in calcium carbonate and contain amino groups originating from chitin and residual proteins. Similar pH_{PZC} values have been reported for crustacean shell-derived materials and chitin-based biosorbents, typically ranging between 7 and 9 depending on the degree of deproteinization, mineral content, and surface treatment [55–57].

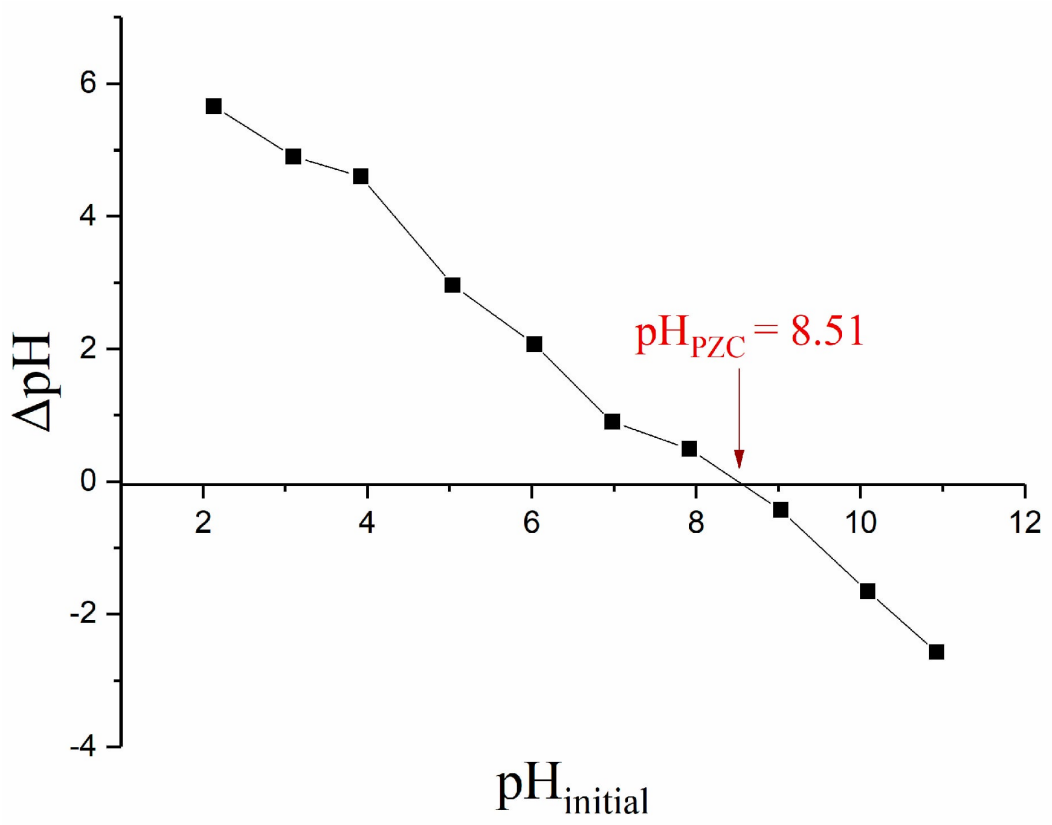

Figure 8. pH_{PZC} of *F. limosus* crayfish shells.

The obtained pH_{PZC} value provides insight into the possible role of surface charge in the adsorption process. Together with the FTIR results and kinetic behavior, these findings suggest that surface complexation and ion-exchange interactions may contribute to metal binding, although additional analyses would be required to confirm the dominant adsorption mechanism.

4. Conclusions

The results of this study demonstrate that shell waste from the invasive crayfish *Faxonius limosus* represents a promising, low-cost biosorbent for the removal of Zn(II) and Cd(II) from aqueous solutions. Material characterization revealed the presence of amino, hydroxyl, amide, and carbonate functional groups together with a predominantly mesoporous structure, providing a heterogeneous organic-mineral matrix capable of interacting with dissolved metal ions.

Batch adsorption experiments showed rapid metal uptake, with equilibrium attained within approximately 60 min. The pseudo-second-order kinetic model provided the best fit for both investigated metal ions, whereas the equilibrium data were best described by the Langmuir model for Cd(II) and the Temkin model for Zn(II). The additional experiments examining operational parameters further demonstrated that metal removal was influenced by both initial solution pH and biosorbent dose. Increasing the biosorbent dose resulted in lower adsorption capacities per unit mass, while its effect on overall removal efficiency differed between the two metals. For Zn(II), removal increased from 76.97% at 1 g/L to 92.73% at 2.5 g/L, with no further improvement at 5 g/L, whereas Cd(II) removal was already high at the lowest tested dose. A dose of 2.5 g/L was therefore selected as a common working dose, enabling direct comparison of Zn(II) and Cd(II) behavior under identical experimental conditions. The pH experiments confirmed the strong influence of solution chemistry on metal removal, although the increased removal observed at higher

pH cannot be attributed exclusively to adsorption because hydrolysis and precipitation may also contribute under these conditions.

Calcium release experiments provided additional insight into the role of the mineral fraction of the shell. Under the same experimental conditions used for metal removal, the mean Ca concentration increased from 50.9 mg/L in the water control to 117.0 mg/L in the presence of Zn(II) and 92.9 mg/L in the presence of Cd(II), corresponding to an additional Ca release of approximately 66.1 and 42.1 mg/L, respectively. These results support the involvement of Ca-containing mineral components in the removal process and suggest that interactions with the carbonate-rich shell fraction contribute to metal uptake. Together with the FTIR results and the determined pHpzc, these findings indicate that Zn(II) and Cd(II) removal by *F. limosus* shells likely involves several concurrent processes, including interactions with surface functional groups, Ca-associated ion-exchange processes, and mineral dissolution-related reactions. However, the available evidence does not allow these individual contributions to be unequivocally distinguished or quantified, and the proposed mechanistic interpretation should therefore be regarded as indicative rather than conclusive.

Overall, the findings demonstrate the potential for valorizing biomass generated during the management of invasive *F. limosus* by converting minimally processed shell waste into a functional biosorbent for metal removal. This approach combines the beneficial use of an underexploited biological waste with a potentially low-cost material for water treatment applications. Further research should focus on experiments with multicomponent systems and real water or wastewater matrices to assess the effects of competing ions, natural organic matter, and ionic strength, while regeneration, metal recovery, and safe management of the spent biosorbent should be investigated to evaluate its practical and environmental feasibility.

Supplementary Materials: The following supporting information can be downloaded at https://www.mdpi.com/article/10.3390/w18202560/s1. Figure S1: FTIR spectra of *F.limosus* crayfish shells. Figure S2: FTIR spectra of crayfish shells loaded with Zn ions. Figure S3: FTIR spectra of crayfish shells loaded with Cd ions.

Author Contributions: Conceptualization, V.V. and D.L.; methodology, T.S. and O.B.; software, O.B.; validation, J.L.S. and T.S.; formal analysis, T.S. and N.P.; investigation, D.L.; resources, V.V. and J.L.S.; data curation, V.V.; writing—original draft preparation, V.V.; writing—review and editing, V.V. and D.L.; visualization, D.L.; supervision, D.L.; project administration, I.Č.; funding acquisition, I.Č. All authors have read and agreed to the published version of the manuscript.

Funding: This research was funded by the Science Fund of the Republic of Serbia (GRANT No. 7417) and the DANUBEcare project "Reducing the negative impact of invasive crayfish *Faxonius limosus* in the Danube by smart exploitation of their meat and shells".

Data Availability Statement: The original contributions presented in this study are included in the article and the Supplementary Materials. Further inquiries can be directed to the corresponding authors.

Acknowledgments: The authors are thankful for the continuous support of the Ministry of Science, Technological Development and Innovation of the Republic of Serbia (contract numbers: 451-03-34/2026-03/200134 and 451-03-33/2026-03/200134).

Conflicts of Interest: The authors declare no conflicts of interest.

References

1. Singh, V.; Singh, N.; Nand Rai, S.; Kumar, A.; Kumar Singh, A.; Singh, M.P.; Sahoo, A.; Shekhar, S.; Vamanu, E.; Mishra, V. Heavy Metal Contamination in the Aquatic Ecosystem: Toxicity and Its Remediation Using Eco-Friendly Approaches. *Toxics* **2023**, *11*, 147. [CrossRef] [PubMed]
2. Mustapha, L.S.; Obayomi, O.V.; Obayomi, K.S. A comprehensive review on potential heavy metals in the environment: Persistence, bioaccumulation, ecotoxicology, and agricultural impacts. *Ecol. Front.* **2026**, *46*, 434–449. [CrossRef]
3. Ghobadifar, V.; Marandi, G.B.; Kurdtabar, M.; Bardajee, G.R. Removal of Pb(II) and Cd(II) ions by MnFe2O4@ Sio2@ VTMS nanocomposites hydrogel from aqueous solutions. *J. Polym. Environ.* **2022**, *31*, 2686–2704. [CrossRef] [PubMed]
4. Karnwal, A. Unveiling the promise of biosorption for heavy metal removal from water sources. *Desalin. Water Treat.* **2024**, *319*, 100523. [CrossRef]
5. Available online: https://www.ipbes.net/ (accessed on 1 June 2026).
6. Available online: https://eur-lex.europa.eu/legal-content/EN/TXT/?uri=CELEX:52020DC0380 (accessed on 1 June 2026).
7. Available online: https://eur-lex.europa.eu/legal-content/EN/TXT/PDF/?uri=CELEX:32014R1143 (accessed on 1 June 2026).
8. Todorov, M.; Trichkova, T.; Hubenov, Z.; Jurajda, P. *Faxonius limosus* (Rafinesque, 1817) (Decapoda: Cambaridae), a New Invasive Alien Species of European Union Concern in Bulgaria. *Acta Zool. Bulg.* **2020**, *72*, 113–121.
9. European Commission. Commission Implementing Regulation (EU) 2016/1141 of 13 July 2016 adopting a list of invasive alien species of Union concern pursuant to Regulation (EU) No 1143/2014 of the European Parliament and of the Council. *Off. J. Eur. Union* **2016**, *L 189*, 4–8. Available online: https://eur-lex.europa.eu/eli/reg_impl/2016/1141/oj/eng (accessed on 1 October 2026).
10. Kaldre, K.; Paaver, T.; Hurt, M.; Gross, R. Continuing expansion of non-indigenous crayfish species in Northern Europe: First established spiny-cheek crayfish Faxonius limosus (Refinesque, 1817) population in Estonia. *BioInvasions Rec.* **2020**, *9*, 127–132. [CrossRef]
11. Zorić, K.S.; Atanacković, A.D.; Ilić, M.D.; Csányi, B.; Paunović, M.M. The Spiny-cheek Crayfish Faxonius limosus (Rafinesque, 1817) (Decapoda: Cambaridae) Invades New Areas in Serbian Inland Waters. *Acta Zool. Bulg.* **2020**, *72*, 623–627.
12. Vijayaraghavan, K.; Palanivelu, K.; Velan, M. Biosorption of copper(II) and cobalt(II) from aqueous solutions by crab shell particles. *Bioresour. Technol.* **2006**, *97*, 1411–1419. [CrossRef] [PubMed]
13. Zhou, C.; Gong, X.; Han, J.; Guo, R. Removal of Pb(II) and Zn(II) from Aqueous Solutions by Raw Crab Shell: A Comparative Study. *Water Environ. Res.* **2016**, *88*, 374–381. [CrossRef] [PubMed]
14. Xiao, Y.; Xue, Y.; Gao, F.; Mosa, M. Sorption of heavy metal ions onto crayfish shell biochar: Effect of pyrolysis temperature, pH and ionic strength. *J. Taiwan Inst. Chem. Eng.* **2017**, *80*, 114–121. [CrossRef]
15. Sun, T.; Xu, Y.; Sun, Y.; Wang, L.; Liang, X.; Jia, H. Crayfish shell biochar for the mitigation of Pb contaminated water and soil: Characteristics, mechanisms, and applications. *Environ. Pollution.* **2021**, *271*, 116308. [CrossRef] [PubMed]
16. Aguilar Torrejón, A.J.A.; Balderas Hernández, P.; Roa Morales, G.; Barrera Díaz, C.E.; Rodríguez Torres, I.; Torres Blancas, T. Relationship, Importance, and Development of Analytical Techniques: COD, BOD, and TOC in Water-An Overview through Time. *SN Appl. Sci.* **2023**, *5*, 118. [CrossRef]
17. Smičiklas, I.D.; Milonjić, S.K.; Pfendt, P.; Raičević, S. The Point of Zero Charge and Sorption of Cadmium(II) and Strontium(II) Ions on Synthetic Hydroxyapatite. *Sep. Purif. Technol.* **2000**, *18*, 185–194. [CrossRef]
18. *ISO 17294-2:2023*; Water Quality. Application of Inductively Coupled Plasma Mass Spectrometry (ICP-MS). Part 2: Determination of Selected Elements, Including Uranium Isotopes. ISO: Geneva, Switzerland, 2023.
19. Tan, K.L.; Hameed, B.H. Insight into the adsorption kinetics models for the removal of contaminants from aqueous solutions. *J. Taiwan Inst. Chem. Eng.* **2017**, *74*, 25–48. [CrossRef]
20. Revellame, E.D.; Fortela, D.L.; Sharp, W.; Hernandez, R.; Zappi, M.E. Adsorption kinetic modeling using pseudo-first order and pseudo-second order rate laws: A review. *Clean. Eng. Technol.* **2020**, *1*, 100032. [CrossRef]
21. Vareda, J.P. On validity, physical meaning, mechanism insights and regression of adsorption kinetic models. *J. Mol. Liq.* **2023**, *376*, 121416. [CrossRef]
22. Musah, M.; Azeh, Y.; Mathew, J.T.; Umar, M.T.; Abdulhamid, Z.; Muhammad, A.I. Adsorption Kinetics and Isotherm Models: A Review. *Caliph. J. Sci. Technol.* **2022**, *4*, 20–26. [CrossRef]
23. Guo, X.; Wang, J. A General Kinetic Model for Adsorption: Theoretical Analysis and Modeling. *J. Mol. Liq.* **2019**, *288*, 111100. [CrossRef]
24. Rajahmundry, G.K.; Garlapati, C.; Senthil Kumar, P.; Alwi, R.S.; Vo, D.N. Statistical Analysis of Adsorption Isotherm Models and Its Appropriate Selection. *Chemosphere* **2021**, *276*, 130176. [CrossRef] [PubMed]
25. Foo, K.Y.; Hameed, B.H. Insights into the Modeling of Adsorption Isotherm Systems. *Chem. Eng. J.* **2010**, *156*, 2–10. [CrossRef]
26. Nebaghe, K.C.; El Boundati, Y.; Ziat, K.; Naji, A.; Rghioui, L.; Saidi, M. Comparison of Linear and Non-Linear Method for Determination of Optimum Equilibrium Isotherm for Adsorption of Copper(II) onto Treated Martil Sand. *Fluid Phase Equilib.* **2016**, *430*, 188–194. [CrossRef]

27. Ayawei, N.; Ebelegi, A.N.; Wankasi, D. Modeling and Interpretation of Adsorption Isotherms. *J. Chem.* **2017**, *2017*, 3039817. [CrossRef]
28. Council of the European Communities. Council Directive 91/271/EEC of 21 May 1991 concerning urban waste-water treatment. *Off. J. Eur. Communities* **1991**, *L 135*, 40–52. Available online: https://eur-lex.europa.eu/eli/dir/1991/271/oj/eng (accessed on 1 October 2026).
29. Kadak, A.E.; Küçükgülmez, A.; Çelik, M. Preparation and Characterization of Crayfish (*Astacus leptodactylus*) Chitosan with Different Deacetylation Degrees. *Iran. J. Biotechnol.* **2023**, *21*, e3253. [CrossRef] [PubMed]
30. Vishali, S.; Rashmi, P.; Karthikeyan, R. Evaluation of Wasted Biomaterial, Crab Shells (*Portunus sanguinolentus*), as a Coagulant in Paint Effluent Treatment. *Desalin. Water Treat.* **2016**, *57*, 13157–13165. [CrossRef]
31. Nwaeju, C.C.; Edoziuno, F.O.; Okuma, S.O.; Tuaweri, T.J. Transforming Marine Waste into Valuable Resources: Morphological and Structural Characterization of Crab Shell Particles for Composite Applications. *BMC Environ. Sci.* **2025**, *2*, 7. [CrossRef]
32. Amelia, R.; Sumiwi, S.A.; Saptarini, N.M.; Levita, J. Chitin Extracted from the Shell of Blue Swimming Crabs (*Portunus pelagicus* Linn.) Inhibits NF-κB p65 in Ethanol-Induced Gastric Ulcerative Wistar Rats. *Mar. Drugs* **2023**, *21*, 488. [CrossRef] [PubMed]
33. Ogresta, L.; Nekvapil, F.; Tămaş, T.; Barbu-Tudoran, L.; Saciu, M.; Hirian, R.; Aluaş, M.; Lazar, G.; Levei, E.; Glamuzina, B.; et al. Rapid and Application-Tailored Assessment Tool for Biogenic Powders from Crustacean Shell Waste: Fourier Transform-Infrared Spectroscopy Complemented with X-ray Diffraction, Scanning Electron Microscopy, and Nuclear Magnetic Resonance Spectroscopy. *ACS Omega* **2021**, *6*, 27773–27780. [CrossRef] [PubMed]
34. Bahadir, T.; Gök, G.; Çelebi, H.; Şimşek, İ.; Gök, O. Seafood Wastes as an Attractive Biosorbent: Chitin-Based Shrimp Shells. *Water Air Soil Pollut.* **2023**, *234*, 1–13. [CrossRef]
35. Jaafarzadeh, N.; Mengelizadeh, N.; Takdastan, A.; Heidari Farsani, M.; Niknam, N.; Aalipour, M.R.; Hadei, M.; Bahrami, P. Biosorption of Heavy Metals from Aqueous Solutions onto Chitin. *Int. J. Environ. Health Eng.* **2015**, *4*, 1–7. [CrossRef]
36. Vijayaraghavan, K.; Ni, H.Y.Y.; Balasubramanian, R. Biosorption Characteristics of Crab Shell Particles for the Removal of Manganese(II) and Zinc(II) from Aqueous Solutions. *Desalination* **2011**, *266*, 195–200. [CrossRef]
37. Faizan, M.; Naz, M.Y.; Shah, S.A.S.A.; Shakir, I.; Khaliq, M.; Busharat, M.A.; Pan, D. Mesoporous Magnetic $MnFe_2O_4$@SiO_2-Chitosan Nanocomposite for Efficient Adsorptive Removal of Zn(II) and Cd(II) Ions from Aqueous Media. *Desalin. Water Treat.* **2025**, *324*, 101488. [CrossRef]
38. Makhlouf, M.R.; Bendjaballah, M.; Boukerche, I.; Kouadri, I.; Hamidoud, S.; Benhamza, M.E.H.; Hammi, H. Eco-Friendly Synthesis of Biosorbent Based on Chitosan-Activated Carbon/Zinc Oxide Nanoparticle Beads for Efficiency Reduction of Cadmium Ions in Wastewater. *Biomass Convers. Biorefin.* **2025**, *15*, 12001–12016. [CrossRef]
39. Rostami, M.S.; Khodaei, M.M. Recent Advances in Chitosan-Based Nanocomposites for Adsorption and Removal of Heavy Metal Ions. *Int. J. Biol. Macromol.* **2024**, *270*, 132386. [CrossRef] [PubMed]
40. Abu El-Soad, A.M.; Lazzara, G.; Abd El-Magied, M.O.; Cavallaro, G.; Al-Otaibi, J.S.; Sayyed, M.I.; Kovaleva, E.G. Chitosan Functionalized with Carboxyl Groups as a Recyclable Biomaterial for the Adsorption of Cu(II) and Zn(II) Ions in Aqueous Media. *Int. J. Mol. Sci.* **2022**, *23*, 2396. [CrossRef] [PubMed]
41. Fernández Pérez, B.; Ayala Espina, J.; Fernández González, M.L.A. Adsorption of Heavy Metals Ions from Mining Metallurgical Tailings Leachate Using a Shell-Based Adsorbent: Characterization, Kinetics and Isotherm Studies. *Materials* **2022**, *15*, 5315. [CrossRef] [PubMed]
42. Tizo, M.S.; Blanco, L.A.V.; Cagas, A.C.Q.; Dela Cruz, B.R.B.; Encoy, J.C.; Gunting, J.V.; Arazo, R.O.; Mabayo, V.I.F. Efficiency of calcium carbonate from eggshells as an adsorbent for cadmium removal in aqueous solution. *Sustain. Environ. Res.* **2018**, *28*, 326e332. [CrossRef]
43. Adeleke, A.O.; Royahu, C.O.; Ahmad, A.; Afolabi, T.T.D.; Alshammari, M.B.; Imteaz, M. A novel oyster shell biocomposite for the efficient adsorptive removal of cadmium and lead from aqueous solution: Synthesis, process optimization, modelling and mechanism studies. *PLoS ONE* **2024**. [CrossRef] [PubMed]
44. Lee, A.Y.W.; Lim, S.F.; Chua, S.N.D.; Sanaullah, K.; Baini, R.; Abdullah, M.O. Adsorption Equilibrium for Heavy Metal Divalent Ions (Cu^{2+}, Zn^{2+}, and Cd^{2+}) into Zirconium-Based Ferromagnetic Sorbent. *Adv. Mater. Sci. Eng.* **2017**, *2017*, 1210673. [CrossRef]
45. Yang, T.; He, R.; Nie, G.; Wang, W.; Zhang, G.; Hu1, Y.; Wu, L. Creation of Hollow Calcite Single Crystals with CQDs: Synthesis, Characterization, and Fast and Efficient Decontamination of Cd(II). *Sci. Rep.* **2018**, *8*, 17603. [CrossRef] [PubMed]
46. Serrano, L.Z.; Lara, N.O.; Vera, R.R.; Cholico-González, D. Removal of Fe(III), Cd(II), and Zn(II) as Hydroxides by Precipitation–Flotation System. *Sustainability* **2021**, *13*, 11913. [CrossRef]
47. Parimal, S.; Prasad, M.; Bhaskar, U. Prediction of Equilibrium Sorption Isotherm: Comparison of Linear and Nonlinear Methods. *Ind. Eng. Chem. Res.* **2009**, *49*, 2882–2888. [CrossRef]
48. Chen, X. Modeling of Experimental Adsorption Isotherm Data. *Information* **2015**, *6*, 14–22. [CrossRef]
49. Zhou, C.; Gong, X.; Zhang, W.; Han, J.; Guo, R.; Zhu, A. Uptake of Cd(II) onto Raw Crab Shells: Isotherm, Kinetic, Adsorption Properties and Mechanisms. *Water Environ. Res.* **2017**, *89*, 817–826. [CrossRef] [PubMed]

50. Jaafarzadeh, N.; Mengelizadeh, N.; Takdastan, A.; Heidari Farsani, M. Adsorption of Zn(II) from Aqueous Solution by Using Chitin Extracted from Crustacean Shells. *J. Adv. Environ. Health Res.* **2014**, *2*, 110–119. [CrossRef]
51. Rahman, A. Promising and Environmentally Friendly Removal of Copper, Zinc, Cadmium, and Lead from Wastewater Using Modified Shrimp-Based Chitosan. *Water* **2024**, *16*, 184. [CrossRef]
52. Morales-Barrera, L.; Cristiani-Urbina, E. Equilibrium Biosorption of Zn^{2+} and Ni^{2+} Ions from Monometallic and Bimetallic Solutions by Crab Shell Biomass. *Processes* **2022**, *10*, 886. [CrossRef]
53. Wierzba, S.; Makuchowska-Fryc, J.; Kłos, A.; Ziembik, Z.; Ochędzan-Siodłak, W. Role of calcium carbonate in the process of heavy metal biosorption from solutions: Synergy of metal removal mechanisms. *Sci. Rep.* **2022**, *12*, 17668. [CrossRef] [PubMed]
54. Chenet, T.; Schwarz, G.; Neff, C.; Hattendorf, B.; Günther, D.; Martucci, A.; Cescon, M.; Baldi, A.; Pasti, L. Scallop shells as biosorbents for water remediation from heavy metals: Contributions and mechanism of shell components in the adsorption of cadmium from aqueous matrix. *Heliyon* **2024**, *10*, e29296. [CrossRef] [PubMed]
55. Nekvapil, F.; Stegarescu, A.; Lung, I.; Hirian, R.; Cosma, D.; Levei, E.; Soran, M.-L. A Novel Nanoporous Adsorbent for Pesticides Obtained from Biogenic Calcium Carbonate Derived from Waste Crab Shells. *Nanomaterials* **2023**, *13*, 3042. [CrossRef] [PubMed]
56. Boudouaia, N.; Bengharez, Z.; Jellali, S. Preparation and Characterization of Chitosan Extracted from Shrimp Shells Waste and Chitosan Film: Application for Eriochrome Black T Removal from Aqueous Solutions. *Appl. Water Sci.* **2019**, *9*, 91. [CrossRef]
57. Chang, J.; Shen, Z.; Hu, X.; Schulman, E.; Cui, C.; Guo, Q.; Tian, H. Adsorption of Tetracycline by Shrimp Shell Waste from Aqueous Solutions: Adsorption Isotherm, Kinetics Modeling, and Mechanism. *ACS Omega* **2020**, *5*, 3467–3477. [CrossRef] [PubMed]

Disclaimer/Publisher's Note: The statements, opinions and data contained in all publications are solely those of the individual author(s) and contributor(s) and not of MDPI and/or the editor(s). MDPI and/or the editor(s) disclaim responsibility for any injury to people or property resulting from any ideas, methods, instructions or products referred to in the content.